archives
of thermodynamics
Vol. **41**(2020), No. 2, 119–146
DOI: 10.24425/ather.2020.133625

Numerical investigation and sensitivity analysis of entropy generation of Al_2O_3/H_2O nanofluid in turbulent regime using response surface methodology

OLATOMIDE G. FADODUN[*a]
BOLANLE A. OLOKUNTOYE[b]
AYODEJI O. SALAU[c]
ADEBIMPE A. AMOSUN[a]

[a] Centre for Energy Research and Development, Obafemi Awolowo University, Ile-Ife Osun state. P.M.B. 13, Ile-Ife, Osun, 220282 Nigeria

[b] Department of Mathematics, Obafemi Awolowo University, Ile-Ife Osun state. P.M.B. 13, Ile-Ife, Osun, 220282 Nigeria

[c] Department of Electrical/Electronic and Computer Engineering, Afe Babalola University, Ado-Ekiti, Nigeria

Abstract This work investigates the effect of Reynolds number, nanoparticle volume ratio, nanoparticle size and entrance temperature on the rate of entropy generation in Al_2O_3 /H_2O nanofluid flowing through a pipe in the turbulent regime. The Reynolds average Navier-Stokes and energy equations were solved using the standard k-ε turbulent model and the central composite method was used for the design of experiment. Based on the number of variables and levels, the condition of 30 runs was defined and 30 simulations were run. The result of the regression model obtained showed that all the input variables and some interaction between the variables are statistically significant to the entropy production. Furthermore, the sensitivity analysis result shows that the Reynolds number, the nanoparticle volume ratio and the entrance temperature have negative sensitivity while the nanoparticle size has positive sensitivity.

Keywords: Entropy production; Reynolds number, Response-surface-methodology; Nanofluid; Single-phase flow

*Corresponding Author. Email: ofadodun@cerd.gov.ng

Nomenclature

$C_{1\varepsilon}$, $C_{2\varepsilon}$, C_μ	–	turbulent constant
c_p	–	specific heat capacity at constant pressure, J/kgK
D_h	–	diameter of the pipe, m
d_f	–	diameter of the water molecule, m
d_p	–	diameter of the nanoparticle, m
f	–	friction factor
G_k	–	rate of production of turbulent kinetic energy, J/kg
h	–	coefficent of heat transfer, W/m^{2}K
I	–	turbulence intensity
k	–	turbulence kinetic energy, m^2/s^2
$(\dot{m})$	–	mass flow rate, kg/s
Nu	–	Nusselt number
T	–	temperature of base fluid, K
Pr	–	Prandtl number of base fluid
Δp	–	pressure drop
q''	–	heat flux at the surface of the pipe
R^2	–	coefficient of determination
Re	–	Reynolds number
Re$_p$	–	nanoparticle Reynolds number
r	–	radial distance, m
S	–	modulus of rate of strain tensor
S_{gen}	–	rate of entropy production
u_r, u_x	–	components velocity, m/s
x	–	axial distance, m
y^+	–	non-dimensionalized wall normal distance

Greek symbols

α	–	thermal diffusivity, m^2/s
ε	–	turbulence energy dissipation, m^2/s^3
λ	–	thermal conductivity, W/m K
μ	–	dynamic viscosity, kg/m s
ρ	–	density of base fluid, kg/m^3
σ_t	–	turbulent constant
σ_k	–	turbulent Prandl number for k
σ_ε	–	turbulent Prandl number for ε
φ	–	nanoparticle volume fraction
κ	–	von Karman constant

Subscripts

in – inlet
nf – nanofluid
p – nanoparticle
f – base fluid
fr – freezing point
t – turbulent

Abbreviations

RSM – response surface methodology

1 Introduction

For many decades, the study of convective heat transfer in thermal systems has received enormous attention from scientists and engineers with a bid to improve the process. This improvement is very crucial as more energy will be saved and also enhance performance [1,2]. Several methods have been proposed to improve the convective heat transfer; among them is replacing the conventional working fluid with nanofluids. Nanofluids are a class of heat transfer fluid created by the suspension of a small amount of nanoscale metallic or non-metallic particles in the base fluid. These hybrid materials have high thermal conductivities and are being considered to be the next-generation heat transfer fluid. The concept was proposed by Choi [3] in 1995 at the Argon National Laboratory when he conducted an experiment on nanofluid and reported enhancements in its thermal conductivity as compared to the base fluid. Other researchers like Eastman [4] and Wang *et al.* [5] worked on Al_2O_3 /H_2O and Cu/ethylene glycol (EG) and reported an increment of about 30–40% in their thermal conductivities.

The enhancement in the convective heat transfer observed by usage of nanofluids has been studied extensively. Sharma *et al.* [6] studied the convective heat transfer of Al_2O_3/H_2O nanofluids in the circular straight pipe and reported a 27.3% increment in its Nusselt number compared to base fluid. Qiang and & Xuan [7] investigated the effect of Reynolds number and volume ratio, on the convective heat transfer of Cu/H_2O nanofluid. The result showed that convective heat transfer was enhanced up to 60% for 2% volume ratio of nanoparticle added. Saha studied the heat transfer and entropy generation in the turbulent regime in TiO_2/H_2O nanofluid flowing in a pipe using a numerical approach. The study revealed that Reynolds number and volume ratio increases the heat transfer process while nanopar-

ticle size suppresses it [8].

Besides the enhancement observed by the usage of nanofluid, it is of paramount importance to perform exergy analysis to reduce entropy production to the lowest possible minimum. Entropy is defined as the measure of the degree of energy lost in the thermal system. It depends mainly on the nature of the fluid, heat transfer and on the flow condition (laminar or turbulent) [9,10]. Minimizing entropy is one of the major aims of thermal design as this will result in an improvement in the amount of energy that can be converted to work (exergy). Several studies using experimental, numerical, and analytical methods have been published on the effect of various parameters on entropy generation by a nanofluid. Konchada *et al.* [11] studied entropy generation of nanofluid containing carbon nanotube in a plum duct with peristalsis using an analytical approach. The entropy generation equation due to viscous and thermal effect was formulated and solved accordingly. The solution showed that entropy generation has a maximum value at the wall of the tube and minimum at the centre. Mah *et al.* [12] investigated the entropy generation rate in Al_2O_3/H_2O nanofluid flowing through a circular microchannel in the laminar flow regime analytically. The results show that thermal irreversibility dominates the entropy generation while the irreversibility due to fluid friction is negligible. Hajialigol *et al.* [13] studied the effect of a magnetic field, viscous and thermal effect on the rate of entropy generation of nanofluid flowing in a three-dimensional microchannel under magnetic field using a numerical approach. The result showed that the thermal effect is the most prominent effect among the three. Ping *et al.* [14] studied the effect of geometry, Reynolds number and volume ratio of volume ratio of Al_2O_3 nanoparticles in the carrier fluid flowing in a microchannel with four different flow control devices (rectangle, V-groove, cylinder and protrusion) on the convective heat transfer and entropy generation. The result showed that microchannels with a cylinder and V-groove control device gave a better heat transfer performance while microchannel with protrusion gave a minimum entropy generation. Amirahmadi *et al.*[15] studied the effect of design parameter on laminar convective heat transfer and exergy analysis of fluid flowing through a trapezoidal duct using a numerical approach. The effects of the beveled corner and surface roughness on the entropy generation were compared. The results showed that both designs reduce entropy production in the trapezoidal duct but vortex generator (surface roughness) performed better as it reduces entropy production by 26.6% while beveled corner reduced it by 8.1%. Bianco *et*

al. [16] studied the effect of duct size, nanoparticle concentration and flow condition on entropy production of Al_2O_3/H_2O nanofluid through a square duct in both laminar and turbulent flow regime subject to constant heat flux at the wall using a numerical approach. The result showed that Bejan number increases with increase in the concentration of the nanoparticle for laminar flow but decreases with an increase in nanoparticle concentration in turbulent flow. Furthermore, the optimum size (diameter of the duct) at which entropy production is at a minimum level in laminar flow is less than the optimum size in turbulent flow. Behera studied the effect of bend angle on pressure drop and entropy generation of Newtonian fluid flowing through a circular bend channel subjected to both constant temperature and constant heat flux boundary conditions at the wall using computational fluid dynamics. Six different bending angles were considered and the result showed that an increment in the bending angle increases the entropy generation of the system [17].

In recent times, researchers have introduced design of experiment (response surface methodology) approach to guide them in order to get a better understanding of heat transfer and entropy production in the nanofluid as many earlier studies were carried out based on one factor at a time analysis which failed to capture the effect of interaction between the input variables on the output variable [18]. Shirvan *et al.* [19] performed a sensitivity analysis of Reynolds number, nanoparticle volume fraction and nanoparticle size on the average Nusselt number of Al_2O_3/H_2O nanofluid flowing through a channel in laminar regime using discrete phase model and response surface methodology. The result showed that Reynolds number and nanoparticle volume fraction have a positive sensitivity to the Nusselt number while nanoparticle size has negative sensitivity. Chan *et al.* [20] investigated the effect of temperature and velocity on the average Nusselt number and Reynolds number of nanofluid flowing through a straight circular pipe with a constant heat flux in the laminar regime using the response surface methodology (RSM). The result showed that both input variables and the interaction between them are significant to the dependent variables. Konchada *et al.* [11] studied the effect of entrance temperature and mass flow rate on entropy generation of Al_2O_3/H_2O nanofluid flowing through a longitudinal fin heat exchanger using computational fluid dynamics. The entropy analysis was carried out using Taguchi technique and the ANOVA (analysis of variance) result showed that both inlet temperature and mass flow rate are statistically significant to the entropy generation

but the effect of inlet temperature is the most profound between the two. Darbari *et al.* [21] performed a sensitivity analysis of Reynolds number, nanoparticle volume ratio and nanoparticle size on the entropy generation of Al_2O_3/H_2O nanofluid flowing through a channel in laminar regime using numerical approach and response surface methodology for the design of experiment. Twenty simulations were performed and the regression model of the entropy production was obtained.

From the review, it can be deduced that the majority of the authors only considered two to three factors at a time in their works carried out using RSM for studying entropy generation in nanofluids. This is due to the fact that as the number of factors increases more experiments will be required to be done. Also, less attention was given to the effect of entrance temperature as the majority of the researchers failed to incorporate it into their study but this has been found to be significant [11]. Furthermore, the majority of the works have focused on the laminar flow condition. Thus, the intention of this work is to undertake a comprehensive study by considering the effect of four input parameters which include: Reynolds number, nanoparticle volume ratio, nanoparticle size and entrance temperature on entropy generation of Al_2O_3/H_2O nanofluid in turbulent flow condition through a pipe. The study will employ the computational fluid dynamic approach using single phase approximation and response surface methodology for the design of the experiment. The outline of the work is as follows: section two enumerate the statement of the problem, section three deals with numerical simulation and validation while section four focus on the results and discussion.

2 Problem statement

The problem under investigation involves entropy production in turbulent forced convection of Al_2O_3 /H_2O nanofluid flowing through a horizontal pipe shown in Fig. 1. The geometry composes of pipe of length 1 m with a diameter of 0.02 m. The fluid enters the pipe with a uniform velocity and temperature. A constant heat flux of 1000 W/m^2 was applied to the wall of the pipe and 0 Pa pressure gauge was imposed on the outlet. The flow and the temperature fields were assumed to be symmetrical about the tube main axis. Thus two-dimensional axisymmetric formulation is employed to simplify the problem.

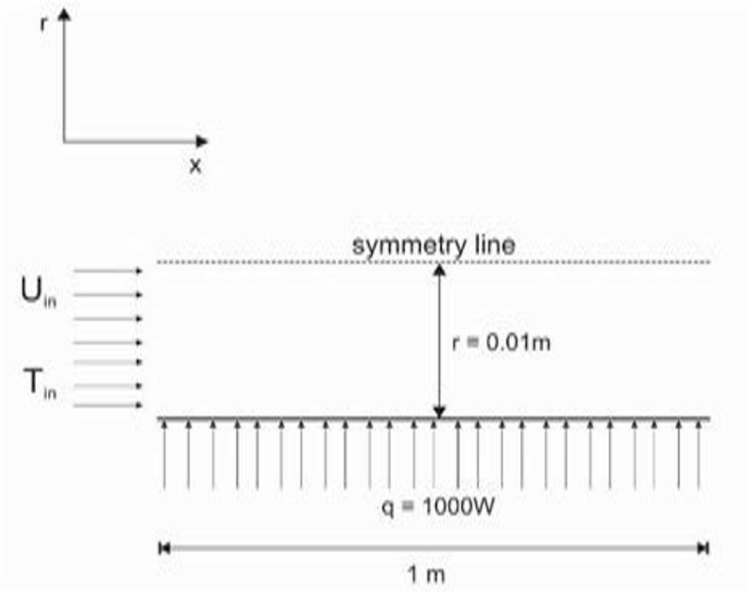

Figure 1: 2D diagram of the model.

2.1 Single phase model

This model assumes the nanoparticle dispersed in the base fluid is fluidized and the resulting suspension can be treated as a single phase fluid. Both nanoparticle and the base fluid are in thermal equilibrium with no slip between them and the thermophysical properties depend on the properties of the base fluid and the nanoparticle [3]. As a result of this, the governing equations (continuity, momentum, and energy equations) applied to the classical Newtonian fluid is also valid for this model.

Assuming the nanofluid is incompressible, the steady state hydrodynamic and heat transfer equations are given as [22]:

$$\frac{\partial u_x}{\partial x} + \frac{\partial u_r}{\partial r} + \frac{u_r}{r} = 0 \ , \tag{1}$$

$$u_x \frac{\partial u_x}{\partial x} + u_r \frac{\partial u_x}{\partial r} = -\frac{1}{\rho_{nf}} \frac{\partial p}{\partial x} + \frac{1}{\rho_{nf}} \left[\frac{1}{r} \frac{\partial}{\partial r} r \left(\mu_{nf} + \mu_t \right) \frac{\partial u_x}{\partial r} \right] + \frac{1}{\rho_{nf}} \frac{\partial}{\partial x} \left[\left(\mu_{nf} + \mu_t \right) \frac{\partial u_x}{\partial x} \right] \ , \tag{2}$$

$$u_r\frac{\partial u_r}{\partial r}+u_x\frac{\partial u_r}{\partial x}=-\frac{1}{\rho_{nf}}\frac{\partial p}{\partial r}+\frac{1}{\rho_{nf}}\frac{1}{r}\frac{\partial}{\partial r}\left[r\left(\mu_{nf}+\mu_t\right)\frac{\partial u_r}{\partial r}\right] +\frac{1}{\mu_{nf}}\frac{\partial}{\partial x}\left[\left(\mu_{nf}+\mu_t\right)\frac{\partial u_r}{\partial x}\right]-\frac{1}{\rho_{nf}}\frac{u_r}{r^2}\,. \tag{3}$$

$$u_x\frac{\partial T_{nf}}{\partial x}+u_r\frac{\partial T_{nf}}{\partial r}=\frac{1}{r}\frac{\partial}{\partial r}r\left(\alpha_{nf}+\alpha_t\right)\frac{\partial T_{nf}}{\partial r}+\frac{\partial}{\partial x}\left(\alpha_{nf}+\alpha_t\right)\frac{\partial T_{nf}}{\partial x}\,, \tag{4}$$

where $\mu_t, \mu_{nf}, \alpha_{nf}$, and α_t are the turbulence viscosity, viscosity of the nanofluid, thermal diffusivity of the nanofluid and turbulence diffusivity respectively. The turbulence viscosity and diffusivity are expressed as:

$$\mu_t=C_\mu\rho\frac{k^2}{\varepsilon}\,, \tag{5}$$

$$\alpha_t=\frac{\mu_t}{\rho_{nf}\sigma_t}\,, \tag{6}$$

where σ_t and C_μ are constants. Using the standard k-ε turbulent model, the equations for turbulent kinetic energy (k) and dissipation rate (ε) are given as:

$$\frac{1}{r}u_r\frac{\partial}{\partial r}\left(rk\right)+u_x\frac{\partial k}{\partial x}=\frac{1}{\rho_{nf}}\frac{1}{r}\frac{\partial}{\partial r}\left[r\left(\mu_{nf}+\frac{\mu_t}{\sigma_k}\right)\right]\frac{\partial k}{\partial r} +\frac{1}{\rho_{nf}}\frac{\partial}{\partial x}\left[\left(\mu_{nf}+\frac{\mu_t}{\sigma_k}\right)\frac{\partial k}{\partial x}\right]+G_k-\rho\varepsilon\,, \tag{7}$$

$$\frac{1}{r}u_r\frac{\partial}{\partial r}\left(r\varepsilon\right)+u_x\frac{\partial \varepsilon}{\partial x}=\frac{1}{\rho}\frac{1}{r}\frac{\partial}{\partial r}\left[r\left(\mu_{nf}+\frac{\mu_t}{\sigma_\varepsilon}\right)\right]\frac{\partial \varepsilon}{\partial r} +\frac{1}{\rho_{nf}}\frac{\partial}{\partial x}\left[\left(\mu_{nf}+\frac{\mu_t}{\sigma_\varepsilon}\right)\frac{\partial k}{\partial x}\right]+G_kC_{1\varepsilon}\frac{\varepsilon}{k}-C_{2\varepsilon}\rho_{nf}\frac{\varepsilon^2}{k}\,, \tag{8}$$

$\sigma_k, \sigma_\varepsilon$ are the turbulent Prandtl number for k and ε, respectively, while G_k represents the rate of production of turbulent kinetic energy given as

$$G_k=\mu_tS^2\,, \tag{9}$$

where $S=\sqrt{2S_{ij}S_{ij}}$ is the modulus of the rate of strain tensor.

The value of the constants used is given in Tab. 1. The inlet turbulence intensity is calculated using the relation

$$I=0.16\mathrm{Re}^{-\frac{1}{8}}\,. \tag{10}$$

Table 1: Values of constants used in k-ε turbulent model.

Constant	$C_{1\varepsilon}$	$C_{2\varepsilon}$	C_μ	σ_k	σ_ε	σ_t	Von Karman
Value	1.44	1.92	0.09	1.0	1.3	0.9	0.4

2.2 Boundary condition

Inlet

$$u_x = u_{in}\ , \quad u_r = 0\ , \quad T = T_{in}\ , \quad k = \frac{3}{2}(I\bar{u})^2\ , \quad \varepsilon = \frac{C_\mu^{0.75}k^{1.5}}{L}\ , \tag{11}$$

where $\bar{u}$ is the velocity scale which is equivalent to inlet velocity u_{in}, L is the turbulence length scale which is taken as the diameter of the pipe and I is the turbulence intensity giving by Eq. (10).

Outlet The parameters u_r, u_x, k, ε, and T were assumed to be fully developed while the atmospheric pressure is taken as 1 Pa:

$$\frac{\partial u_r}{\partial x} = 0, \quad \frac{\partial u_x}{\partial x} = 0, \quad \frac{\partial T}{\partial x} = 0, \quad \frac{dk}{dx} = 0, \quad \frac{d\varepsilon}{dx} = 0, \quad P_{gauge} = 0 \text{ Pa}\ . \tag{12}$$

Wall The no-slip condition constraint is invoke:

$$u_x = 0\ , \quad u_r = 0\ , \quad q = 1000 \text{ W/m}^2\ . \tag{13}$$

Symmetry

$$\frac{\partial u_r}{\partial r} = 0\ , \quad \frac{\partial T}{\partial r} = 0\ . \tag{14}$$

2.3 Wall treatment

At the near wall region, there is a high fluctuation of turbulent quantities ($\bar{u}, u'$, k, and ε) (i.e., average velocity , turbulent velocity component, turbulent kinetic energy and turbulent dissipation) which are not captured by the k-ε model. As a result, the empirical model's wall function which satisfies the physics of the flow was applied to represent conditions near the wall. The law of the wall says that the mean velocity at a point p is proportional to the distance y_p from the wall [23]. This is expressed mathematically as

$$u^+ = \frac{1}{\kappa}\ln y^+ \ = \frac{1}{\kappa}\ln\left(\frac{\rho\ C_\mu^{0.25}k_p y_p}{\mu}\right), \tag{15}$$

where k_p is the turbulent kinetic energy at an arbitrary point p, y_p is the distance from an arbitrary point p to the wall, ρ is the density of the fluid, μ is the viscosity of the fluid, C_μ constant of turbulent and κ von Karman constant and y^+ is the dimensionless normal distance from the wall. For k-ε model, the range of y^+ is giving as $30 \leq y^+ \leq 300$.

2.4 Thermophysical properties of the water

Kay and Crawford gave correlation for density, viscosity, heat capacity and thermal conductivity of water in term of temperature:

$$\rho_f = 330.12 + 5.92T - 1.63 \times 10^{-2}T^2 + 1.33 \times 10^{-5}T^3 \,, \tag{16}$$

$$c_p = 10^{-3}\left(10.01 - 5.14 \times 10^{-2}T + 1.49 \times 10^{-4}T^2 - 1.43 \times 10^{-7}T^3\right) \,, \tag{17}$$

$$\mu_f = 0.00002414 \times 10^{\left(\frac{247.81}{T-140}\right)} \,, \tag{18}$$

$$k_f = 0.76761 + 0.53211 \times 10^{-3}T - 0.98244 \times 10^{-5}T^2 \,. \tag{19}$$

2.5 Single phase model for nanofluid thermophysical properties

Assuming the nanoparticles are uniformly dispersed in the base fluid the resulting density can be estimated using Pak and Cho's relation [25]

$$\rho_{nf} = (1-\varphi)\,\rho_{bf} + \varphi\rho_{np} \,. \tag{20}$$

The resultant heat capacity of the nanofluid is calculated using Xuan and Roetzel relation[26] given as

$$c_{pnf} = \frac{(1-\varphi)\,(\rho c_p)_{bf} + \varphi(\rho C)_{np}}{\rho_{nf}} \,. \tag{21}$$

Corcione empirical formulas [27] were used to estimate the thermal conductivity and the viscosity of the nanofluid given as:

$$\frac{\mu_f}{\mu_{nf}} = 1 - 34.87\left(\frac{d_p}{d_f}\right)^{-0.3}\varphi^{1.03} \,, \tag{22}$$

$$\frac{\lambda_{nf}}{\lambda_f} = 1 + 4.4\mathrm{Re}_p^{0.4}\mathrm{Pr}_f^{0.66}\left(\frac{T_{nf}}{T_{fr}}\right)^{10}\left(\frac{k_{np}}{k_f}\right)^{0.33}\varphi^{0.66} \,, \tag{23}$$

here $d_f = 0.1\left(\frac{6M}{N\pi\rho_f}\right)$, $\mathrm{Re}_p = \frac{2\rho_f K_b T_{nf}}{\pi\mu_f^2 d_p}$, and d_f,, d_p, M, and K_b are the diameter of the water molecule, the diameter of Al_2O_3 nanoparticle, the molecular mass of water and Boltzmann constant, respectively.

The thermophysical properties of Al_2O_3 are shown in Tab. 2. Note all the thermophysical properties of the nanofluid are evaluated at the entrance temperature [28].

Table 2: Properties of Al_2O_3 [8].

Parameters	c_p(J/K)	ρ (kg/m^3)	λ (W/m K)
Value	765	3970	42

2.6 Heat transfer and entropy generation

The Reynolds is defined as

$$\mathrm{Re} = \frac{\rho D_h u_{mean}}{\mu} , \tag{24}$$

where u_{mean}, D_h are the mean velocity and hydraulic diameter, respectively.

The Darcy friction factor for turbulent flow is given as

$$f = \frac{2D_h \Delta p}{\rho u_{mean}^2 H} , \tag{25}$$

where H is the length of the pipe.

The mean velocity u_{mean} is defined as

$$u_{mean} = \frac{2}{R^2}\int_0^R u\,(x,r)\; r dr . \tag{26}$$

The heat transfer coefficient $h(x)$ is given as

$$h\,(x) = \frac{q}{T_{wall} - T_{bulk}} , \tag{27}$$

where q is the heat flux at the surface of the pipe and the bulk temperature (T_{bulk}) is calculated using the following relation:

$$T_{bulk}\,(x) = T\,(x_0) + \frac{\dot{q}_s \pi D_h x}{\dot{m} c_p} . \tag{28}$$

The Nusselt number is given as

$$\mathrm{Nu}(x) = \frac{h(x)D}{k}. \tag{29}$$

The mean Nusselt number is evaluated using Simpson's 1/3 rule given as

$$\mathrm{Nu}_{ave} = \frac{1}{x_{out} - x_{in}} \int_{x_{in}}^{x_{out}} \mathrm{Nu}(x)dx \ . \tag{30}$$

Note that the initial point (x_{in}) is taken as 0.4 m, while $x_{out} = 1$ m. At this initial point, the flow is assumed to be fully developed [29]. The entropy generation is calculated using the Ratt and Raut expression [30]

$$S_{gen} = \frac{\pi D_h^2 q^2 L}{\lambda_{nf} \mathrm{Nu}_{ave} T_{ave}} + \frac{32\,\dot{m}^3 f L}{\rho_{nf}^2 \pi^2 D_h^5 T_{ave}} \ , \tag{31}$$

where $\dot{m}$ is the mass flow rate, q is the constant heat flux, L is the length of the pipe, λ_{nf} the thermal conductivity of the nanofluid, ρ_{nf} the density of the nanofluid, f friction factor, Nu_{ave} average Nusselt number, D_h hydraulic diameter, and T_{ave} is the average temperature calculated using

$$T_{ave} = \frac{T_{in} - T_{out}}{\ln \frac{T_{in}}{T_{out}}} \ . \tag{32}$$

The mass flow rate through a circular pipe is calculated using

$$\dot{m} = \frac{\mathrm{Re}\ \mu D_h}{4} \ . \tag{33}$$

The procedure to calculate the entropy generation using Eq. (30) is as follows:

1. The quantities ρ_{nf} and λ_{nf} for each run will be calculated using Eqs. (20) and (23), respectively.
2. The average Nusselt number (Nu), friction factor (f) and average exit temperature (T_{out}) is also calculated using Eq. (28).
3. The average temperature (T_{ave}) will be calculated using Eq. (32).
4. The mass flow rate ($\dot{m}$) will be obtained using Eq. (33). The remaining values of the terms needed are as follows:
   $q = 1000$ W/m^2, $D_h = 0.02$ m, L $= 1$ m, $\pi = 3.142$.

3 Numerical solution

The Reynolds-averaged Navier-Stokes (RANS) model for continuity, momentum, energy and the turbulent equations are solved with the boundary condition stated above using finite volume commercial engineering simulation software program (Adina) [31]. The SIMPLE (semi-implicit method for pressure linked equations) algorithm is used for pressure-velocity coupling and the second-order upwind scheme was applied to discretize convection term in the equations. Gauss-Seidel approach was used to solve for the temperature, velocity and turbulent terms. The iterative procedure was terminated when the convergence criteria are satisfied (the residual for all the equations is less than 10^{-6} and the residual for solutions variables is less than 10^{-5}). A square mesh composed of four nodes was used. The mesh size increases progressively from the wall along the radii direction in order to capture the rapid change in velocity and temperature that occur at the boundary layer [32,33].

3.1 Response surface methodology

Response surface methodology (RSM) is a set of advanced design of experiments (DOE) technique that helps us have a better understanding of the relationship between the input variables and the response. It makes use of statistical and mathematical methods to build an empirical model that could fit the experimental data [34]. The multivariate model for the output variable is gives as

$$y = \alpha_0 + \sum_{i=1}^{4} \alpha_i x_i + \sum_{i=1}^{4} \alpha_{ii} x_i x_i + \sum_{i=1}^{4} \alpha_{ij} x_i x_j \ , \tag{34}$$

where α_0, α_i, α_{ii}, and α_{ij} are the intercept, linear regression coefficient of ith factor, quadratic regression coefficient of ith factor and intercept of ith and jth factor, respectively. Response surface methodology can be performed using either Box-Behnken design or central composite design. The former has fewer design points than the latter thus less expensive to do. However, it is not suited for the sequential experiment as it does not have an embedded factorial. Thus, this study employed the central composite design method to study, the effect of four variables: Reynolds number, nanoparticle volume ratio, nanoparticle size and entrance temperature on the rate of entropy generation. Each factor is set to 5 levels (the range of interest for each variable is divided into five equal parts) with an alpha value

(calculated using $\alpha = (2^k)^{0.25}$, where k = number of variables considered) set to 2. Based on the number of variables and levels, the condition of 30 runs are defined which consist of 16 factorial points, 8 axial points and 6 centre points [35,36]. Table 3 shows the variable and the value associated with each level The RSM analysis will be carried out using Design Expert statistical software package, that is specifically dedicated to performing design of experiments (DOE) [37].

Table 3: Variable and the value associated with each level use in response surface methodology.

Variable	Unit	Level				
		-2	-1	0	1	2
Reynolds number, Re		7000	7200	7400	7600	7800
Temperature, T	K	290	300	310	320	330
Diameter, d_p	1×10^{-9} m	20	40	60	80	100
Volume ratio, φ	%	1	2	3	4	5

Note: d_p is the diameter of the nanoparticle and φ is the ratio of nanoparticle in water

3.2 Validation and grid dependence

Grid sensitivity test was carried out by varying the number of grids used in both axial and radial direction to subdivide the domain using water at Reynolds number of 6500 as a benchmark. Several combinations were used until we obtained a stable one ($N_r = 100$ by $N_x = 500$, where N_r and N_x denote the number of grid points in radial and axial directions, respectively) in which further increase in the number of grids at both axial and radial direction does not change the value of average Nusslet number more than 1.5%. The accuracy of the grid combination chosen was further validated by estimating the average Nusselt number of pure water for a range of Reynolds number (5000 to 12 000) and compared the result with Gnielinski correlation [38]

$$\mathrm{Nu} = \frac{\frac{f}{8}\left(\mathrm{Re} - 1000\right)\mathrm{Pr}}{1 + 12.7\left(\frac{f}{8}\right)^{0.5}\left(\mathrm{Pr}^{\frac{2}{3}} - 1\right)}\left[1 + \left(\frac{d}{L}\right)^{\frac{2}{3}}\right], \tag{35}$$

where $f = (0.79\ln \mathrm{Re} - 1.64)^{-2}$ and $\mathrm{Pr} = \frac{\mu c_p}{k}$ is the Prandtl number. The result falls between -10% to 15% of the Gnielinski correlation as shown in

Fig. 2. Furthermore, the friction factor for various Reynolds number was estimated using Darcy friction factor and the result was compared with the work of Saha [8] and Blasius correlation[39] given by Eq.(36). Figure 3 show that there is a good agreement among them.

$$f = \frac{0.316}{\mathrm{Re}^{0.25}} \,. \tag{36}$$

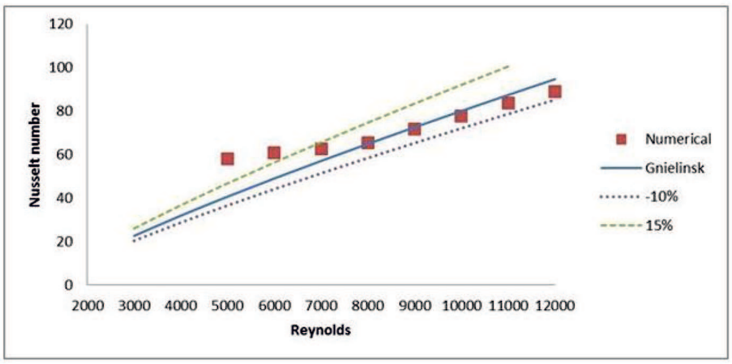

Figure 2: Comparison of the average Nusselt number with Gnielinski correlation.

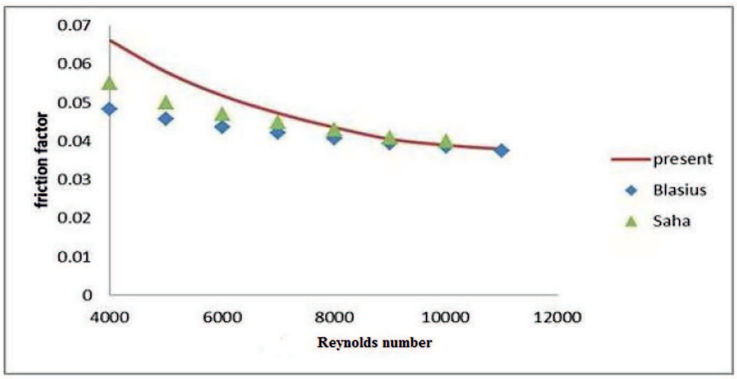

Figure 3: Comparison of the friction factor.

4 Result and discussion

The effect of four input parameters: Reynolds number (Re), volume ratio (φ), nanoparticle diameter (d_p) and entrance temperature (T_{ent}) of AlO_3/H_2O nanofluid flowing through a pipe on the rate of entropy production rate (S_{gen}) has been investigated. The result of 30 runs performed with the corresponding entropy production rate is shown in Tab. 4.

Table 4: The levels of the factors and the result of the entropy generation.

Run no.	Re	φ	d_p	T	S_{gen}
1	-1	-1	-1	-1	6.38E-01
2	1	-1	1	-1	6.43E-01
3	-1	1	-1	-1	6.12E-01
4	1	1	-1	-1	6.06E-01
5	-1	-1	1	1	5.59E-01
6	0	0	0	0	5.80E-01
7	-2	0	0	0	5.86E-01
8	-1	1	1	1	5.28E-01
9	1	1	-1	1	4.98E-01
10	-1	-1	-1	1	5.42E-01
11	1	-1	-1	-1	6.32E-01
12	0	0	0	0	5.80E-01
13	1	1	1	1	5.22E-01
14	0	0	-2	0	5.48E-01
15	-1	1	-1	1	5.03E-01
16	0	0	0	-2	6.80E-01
17	0	-2	0	0	6.14E-01
18	-1	-1	1	-1	6.49E-01
19	0	0	0	0	5.80E-01
20	0	0	0	0	5.80E-01
21	1	-1	-1	1	5.36E-01
22	2	0	0	0	5.74E-01
23	0	0	2	0	5.91E-01
24	0	0	0	2	4.83E-01
25	1	-1	1	1	5.54E-01
26	1	1	1	-1	6.22E-01
27	0	0	0	0	5.80E-01
28	0	2	0	0	5.64E-01
29	0	0	0	0	5.80E-01
30	-1	1	1	-1	6.29E-01

4.1 Rate of entropy generation

Table 5 shows the summary of the model, it reveals that a quadratic model with the coefficient of determination (R-squared or R^2) of 0.9992, adjusted R^2 ($R^2{}_{adj}$) of 0.9985 and predicted R^2 ($R^2{}_{pre}$) of 0.9954 is the best to fit the simulation data. The R^2 value represents how close the simulation data to regression line, $R^2{}_{adj}$ represents a modified version of R^2 that has been adjusted based on the number of independent variables while the $R^2{}_{pre}$ estimates the predictive capability of the model. The difference between $R^2{}_{adj}$ and $R^2{}_{pre}$ was found to be less than 0.2 which indicates the suitability of the model [40]. To verify the accuracy of the model generated and determine the factors that are statistically significant, analysis of variance (ANOVA) was performed based on the confidence level of $\alpha = 0.05$.

Table 5: Summary of the model used to fit mean entropy generation.

Model	P-value	R^2	$R^2{}_{adj}$	$R^2{}_{pre}$	DoF*	Remark
Linear	<0.0001	0.9898	0.9882	0.9841	4	–
2FI**	0.1603	0.9935	0.9900	0.9887	6	–
Quadratic	<0.0001	0.9992	0.9985	0.9954	4	suggested
Cubic	<0.0001	1.0000	1.0000	0.9985	8	aliased
Residual	–	–	–	–	7	–

*Dof – degree of freedom, **2FI – sequential sum of squares for the two-factor interaction

Table 6 showed the summary of the ANOVA after terms that were not statistically significant (P-value > 0.005) have been removed. The model F-value which compares the variance of the model to residual's variance is 2417.21 and P-value which is a measure the probability of obtaining null hypothesis (that is none of the input variables has an effect on the entropy) is less than 0.0001, the low P-value made us reject the null hypothesis. The model means square (estimate population variance which is the ratio of the sum of the square to the degree of freedom) was 0.007 [41]. The adeq-precision (this compares the range of predicted value at the design point to prediction error) gave a value of 196 [42]. All these values indicate that the model obtained is good enough to fit the simulation data. Also, it is shown that all the input variables, namely Reynolds number, volume ratio, nanoparticle diameter and entrance temperature, and some interactions among them such as volume ratio – entrance temperature, volume

ratio – nanoparticle size, nanoparticle size – entrance temperature, are all statistically significant.

Table 6: Results of ANOVA.

	Sum of square	Degree of freedom	Mean square	F-value	P-value
Models	0.066	9	7.334E-003	2417.21	< 0.0001
A-Reynolds	2.170E-004	1	2.170E-004	71.53	< 0.0001
B-volume ratio	4.633E-003	1	4.633E-003	1527.03	< 0.0001
C-diameter	2.150E-003	1	2.150E-003	708.58	< 0.0001
D-Temperature	0.058	1	0.058	19245.68	< 0.0001
B^2	1.347E-004	1	1.347E-004	44.39	< 0.0001
C^2	1.980E-004	1	1.980E-004	65.26	< 0.0001
BC	4.186E-005	1	4.186E-005	13.80	0.0014
BD	1.458E-004	1	1.458E-004	48.05	< 0.0001
CD	5.181E-005	1	5.181E-005	17.08	0.0005
Residual	6.068E-005	20	3.034E-006		
Lack of Fit	6.068E-005	15	4.045E-006		
Pure Error	0.000	5	0.000		
Total	0.066	29			

$R^2 = 0.9992$, ${R^2}_{adj} - {R^2}_{pre} = 0.0024$, Adeq. precision = 196.192

The regression model obtained for the entropy generation number is given as

$$S_{gen}\,(\mathrm{Re}, \varphi, T, d_p) = 0.58 - 0.003\mathrm{Re} - 0.013894\varphi + 0.00946 d_p - 0.049T + 0.002176\varphi^2 - 0.00264 d_p^2 + 0.0016\varphi d_p - 0.003019\varphi T + 0.0018 d_p T. \quad (37)$$

This equation is valid for $7000 \leq \mathrm{Re} \leq 7800$, $0.01 \leq \varphi \leq 0.05$, 20 nm $\leq d_p \leq 100$ nm, 290 K $\leq T \leq 330$ K. Figure 4 shows the three-dimensional and contour graphs of entropy production rate as a function of Reynolds number and nanoparticle concentration when the entrance temperature and nanoparticle size were kept at level 0. It showed that the maximum entropy production rate occurred at ($\mathrm{Re} = -2$, $\varphi = -2$). This indicates that entropy production decreases as Reynolds number and nanoparticle concentration increase. This is expected as an increment in Reynolds number and nanoparticle concentration enhance the convective heat transfer (Nu) and in turn reduce thermal entropy production rate. Figure 5 shows the 3D and contour graphs of entropy production as a function of nanoparticle

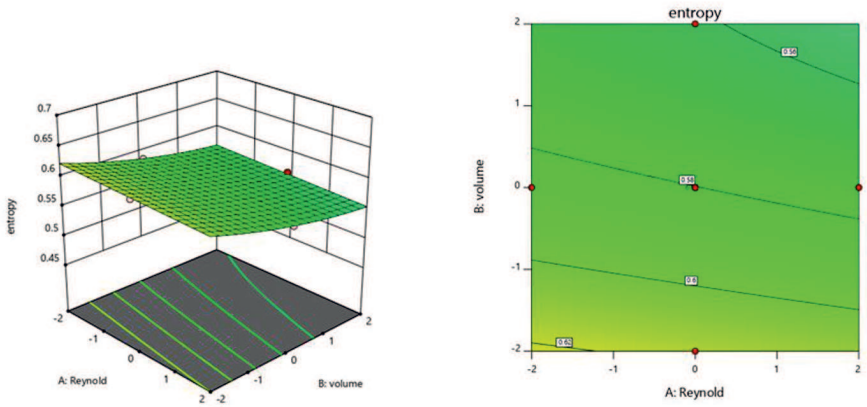

a) b)

Figure 4: a) 3D graph of entropy production against Reynolds number and volume ratio of nanoparticle, b) contour graph of entropy production against Reynolds number and volume ratio of nanoparticle.

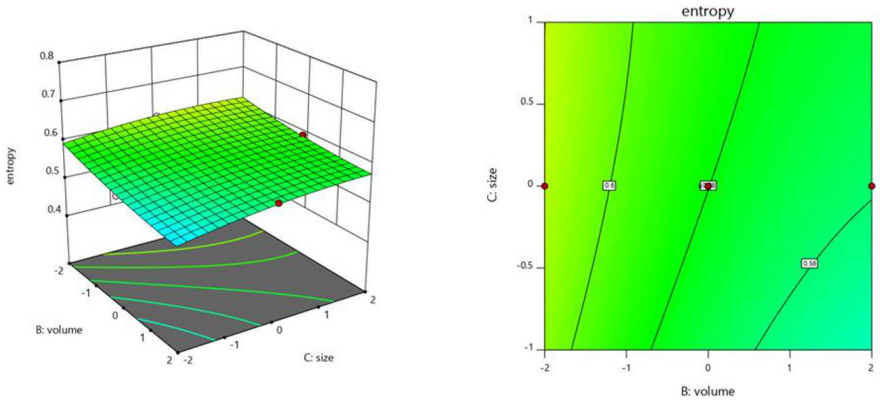

a) b)

Figure 5: a) 3D graph of entropy production against volume ratio of nanoparticle and nanoparticle size, b) contour graph of entropy production against volume ratio of nanoparticle and nanoparticle size.

concentration and nanoparticle size when Reynolds number and entrance temperature were set at the level 0. It showed that the maximum value was found at ($\varphi = -2$, $d_p = 2$). This also is expected as the decrease in

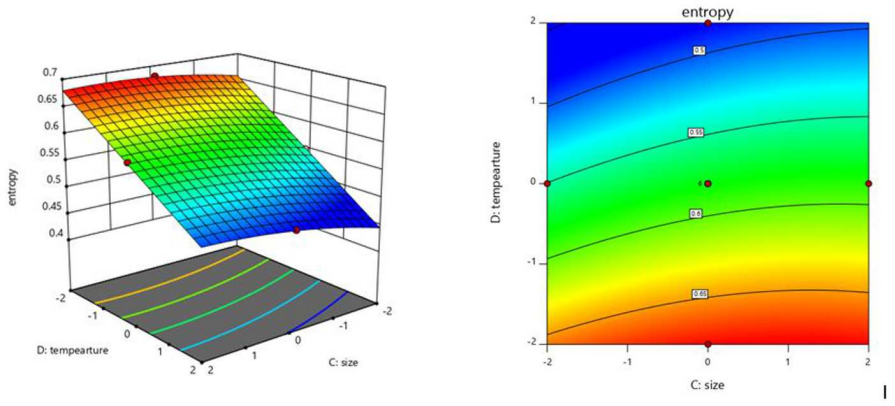

a) b)

Figure 6: a) 3D graph of entropy production against entrance temperature and nanoparticle size, b) contour graph of entropy production against entrance temperature and nanoparticle size.

nanoparticle concentration enhances entropy production as discuss earlier while the increase in nanoparticle size will cause a reduction in Brownian motion which results in the decrease in Nusselt number and in turn increase the entropy production rate. Figure 6 shows the graphs of entropy production rate as a function of nanoparticle size and entrance temperature when Reynolds number and nanoparticle concentration were set at level 0. The graph shows the maximum value at ($d_p = 2$, $T_{ent} = -2$ K). This implies that an increase in entrance temperature decreases the entropy production rate.

4.2 Test of residual

The residual of the model was further examined to ascertain its accuracy. Figure 7 shows the normality plot of residual which was used to confirm the normality of the assumption [43]. The graph revealed that the majority of the simulation data either fall on the line or close to the line. This indicates that the model is good to predict the output variable (entropy generation). Figure 8 shows the plot of studentized residual against the predicted value which was used to check non-linearity, constant variance assumption and outlier [44]. The plot showed two attributes; all the data points are within the three sigma limit. Also, the data scatter without any trend. These

validate the suitability of the model. Furthermore, Fig. 9 showed the plot of residuals against the number of runs. The plot shows no trend as it confirms the independence assumption and lastly, Fig. 10 shows the plot of predicted value against actual values. The points fell on the straight line confirming that the regression model gave a good prediction of the simulation result.

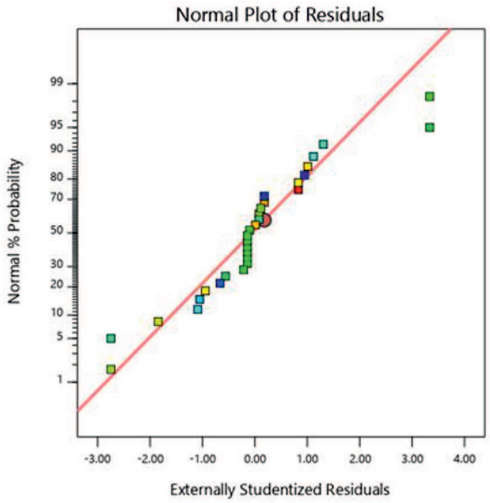

Figure 7: Graph of normality against residual for entropy production.

4.3 Sensitivity analysis

Carrying out sensitivity analysis is important as it avails us the opportunity to determine the effect of input variables on the output variable under certain condition. One way of achieving this is by taking the partial derivative of the output variable's function with respect to input variables [45,46,47]. Here, the partial derivative of the regression model for entropy generation rate with respect to all the four input parameter are given as:

$$\frac{\partial S_{gen}}{\partial \mathrm{Re}} = -0.003 \,, \tag{38}$$

$$\frac{\partial S_{gen}}{\partial \varphi} = -0.014 + 0.004352\varphi + 0.00161 d_p - 0.003019 T \,, \tag{39}$$

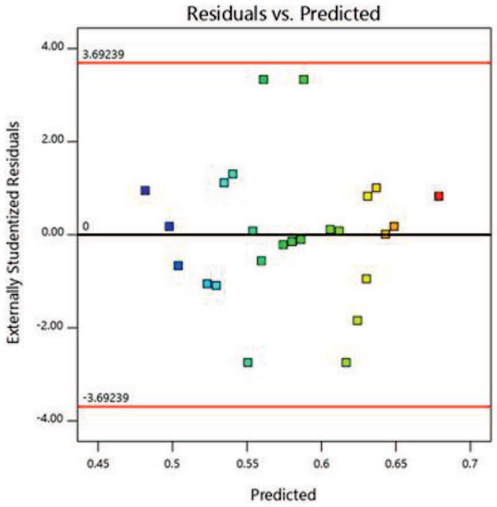

Figure 8: Graph of studentized residual against the predicted value for entropy production.

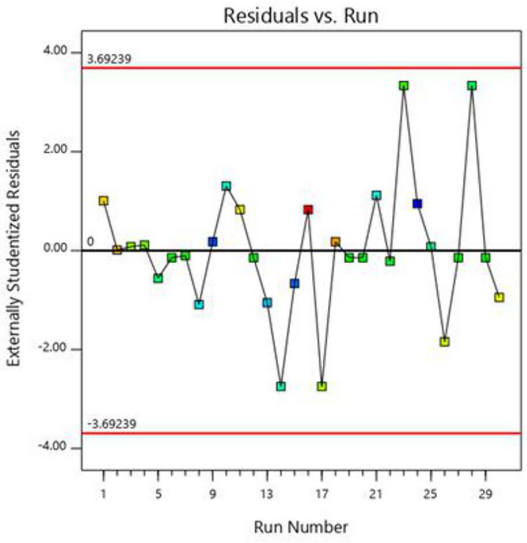

Figure 9: Graph of residuals against the number of runs for entropy production.

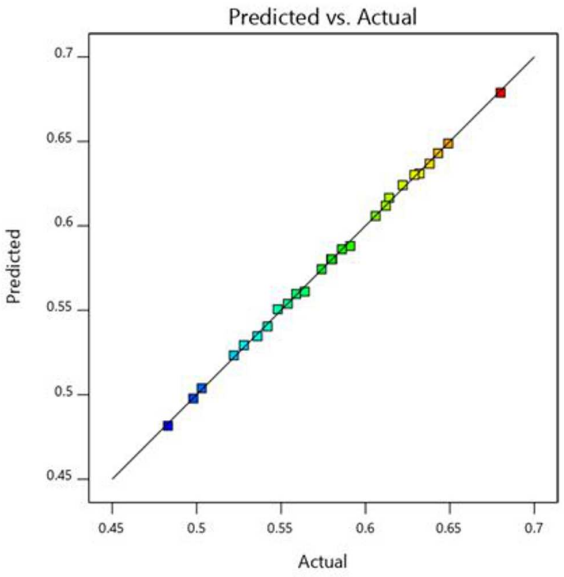

Figure 10: Graph of predicted value against actual values.

$$\frac{\partial S_{gen}}{\partial d_p} = 0.00946 - 0.00408 d_p + 0.00161\varphi + 0.0018T \ , \tag{40}$$

$$\frac{\partial S_{gen}}{\partial T} = -0.049 - 0.003019\varphi + 0.0018 d_p \ . \tag{41}$$

Table 7 shows the result of the sensitivity of the rate of entropy production for various configurations to the input variables. The positive value of the sensitivity connotes an increment in the observable output variable with respect to increment in the input variable, while a negative value implies the opposite. Entrance temperature (T_{ent}) has the highest sensitivity occurred at (Re = 1, $\varphi = 2$, $d_p = -1$, $T_{in} = 0$) followed by nanoparticle volume ratio (φ) at (Re = 1, $\varphi = -2$, $d_p = -1$, $T_{in} = 0$), nanoparticle size (d_p) at (Re = 1, $\varphi = 1$, $d_p = -1$, $T_{in} = 0$) and lastly Reynolds number whose sensitivity is constant throughout all configurations. Furthermore, both volume ratio and entrance temperature have negative sensitivities, this implies that the increase in their values will result in a decrease in the rate of entropy production while the increase in nanoparticle size will increase the rate of entropy production for all configurations.

Table 7: Sensitivity analysis of the rate of entropy production.

Variables				Sensitivity			
Re	φ	d_p	T	Re	φ	d_p	T
-2	-1	0	1	-0.003	-0.0213	0.0095	-0.046
-1	-1	0	1	-0.003	-0.0213	0.0095	-0.046
0	-1	0	1	-0.003	-0.0213	0.0095	-0.046
1	-1	0	1	-0.003	-0.0213	0.0095	-0.046
2	-1	0	1	-0.003	-0.0213	0.0095	-0.046
1	-2	-1	0	-0.003	-0.0242	0.0115	-0.045
1	-1	-1	0	-0.003	-0.0199	0.0135	-0.048
1	0	-1	0	-0.003	-0.0156	0.0155	-0.051
1	1	-1	0	-0.003	-0.0113	0.0175	-0.054
1	2	-1	0	-0.003	-0.007	0.0095	-0.057
0	1	-2	-1	-0.003	-0.0099	0.0135	-0.056
0	1	-1	-1	-0.003	-0.0083	0.0095	-0.054
0	1	0	-1	-0.003	-0.0067	0.0055	-0.052
0	1	1	-1	-0.003	-0.0051	0.0015	-0.05
0	1	2	-1	-0.003	-0.0035	0.0095	-0.048
-1	0	1	-2	-0.003	-0.0064	0.0035	-0.047
-1	0	1	-1	-0.003	-0.0094	0.0055	-0.047
-1	0	1	0	-0.003	-0.0124	0.0075	-0.047
-1	0	1	1	-0.003	-0.0154	0.0095	-0.047
-1	0	1	2	-0.003	-0.0184	0.0095	-0.047

5 Conclusion

The convective heat transfer in Al_2O_3/H_2O nanofluid flowing through a pipe was investigated using the numerical approach and the response surface methodology (RSM) to unravel the effect of four parameters, namely Reynolds number, volume ratio, nanoparticle size and the entrance temperature on the rate of entropy production. The numerical approach employed the single-phase model for thermophysical properties and central composite design method for design of the experiment. Based on the number of variables and levels, the conditions for 30 runs were defined. The result

showed that all the input variables and some interactions between them (volume ratio – entrance temperature, volume ratio – nanoparticle size, and nanoparticle size – entrance temperature) are statistically significant to the rate of entropy generation. Furthermore, a sensitivity analysis was performed on the regression model generated for the rate of entropy generation. The results obtained are summarized below:

- Increase in Reynolds number, nanoparticle concentration and entrance temperature decrease the entropy production for all configurations.
- Increase in nanoparticle size enhances entropy production rate for all configurations.
- Entrance temperature is the most sensitive parameter.
- Reynolds number has constant sensitivity for all configurations.

Received 11 May 2018

References

[1] Yousefi S.A., Sharifpur M., Meyer J.P.: *The effects of uncertainly of nanolayer properties on the heat transfer through nanofluids.* In Proc. 10th Int. Conf. on Heat Transfer, Fluid Mechanics and Thermodynamics (HEFAT 2014), Orlando, July 14–16, 2014.

[2] Eapen J. Rusconi R., Piazz R., Yip S.: *The classical nature of thermal conduction in nanofluids.* J. Heat Transf. **132**(2010), 10, 102402.

[3] Choi S.U.S.: *Enhancing thermal conductivity of fluids with nanoparticles.* In: Developments and Applications of Non-Newtonian Flows (D.A. Siginer, H.P. Wang, Eds.). ASME FED-Vol.2 31/MD-Vol. 66, New York 1995, 99–105.

[4] Eastman J.A., Choi S.U.S., Li S., Yu W., Thompson L.J.: *Anomalously increased effective thermal conductivities of ethylene glycol-based nanofluids containing copper nanoparticles.* Appl. Phys. Lett. **78**(2001), 6, 718–720.

[5] Wang X.Q., Mujumdar A.S.: *Heat transfer characteristics of nanofluids*: *A review.* Int. J. Therm. Sci. **46**(2007), 1, 1–19.

[6] Sharma K.V., Sundar L.S., Sarma P.K.: *Estimation of heat transfer coefficient and friction factor in the transition flow with low volume concentration of* Al_2O_3 *nanofluid flowing in a circular tube and with twisted tape insert.* Int. Commun. Heat Mass **36**(2009), 5, 503–507.

[7] Li Q., Xuan Y.: *Convective heat transfer and flow characteristics of Cu-water nanofluid.* Science in China E: Technol. Sci. **45**(2002), 4, 408–416.

[8] Saha G., Paul M.C.: *Numerical analysis of the heat transfer behaviour of water-based Al2O3 and TiO2 nanofluids in a circular pipe under the turbulent flow condition*. Int. Commun. Heat Mass **56**(2014), 96–108.

[9] Li P., Xie Y., Zhang D., Xie G.: *Heat transfer enhancement and entropy generation of nanofluids laminar convection in microchannels with flow control devices*. Entropy **18**(2016), 4, 134.

[10] Rashidi S., Bovand M., Esfahani J.A.: *Sensitivity analysis for entropy generation in porous solar heat exchangers by RSM*. J. Thermophys. Heat Tr. **31**(2016), 2, 390-402.

[11] Konchada P.K., Vinay P.V., Bhemuni V.: *Statistical analysis of entropy generation in longitudinally finned tube heat exchanger with shell side nanofluid by a single phase approach*. Arch. Thermodyn. **37**(2016), 3, 3–22.

[12] Mah W.H.: Hung Y.M., Guo N.: *Entropy generation of viscous dissipative nanofluid flow in microchannels*. Int. J. Heat Mass Tran. **55**(2012), 15-16, 4169–4182.

[13] Hajialigol N., Fattahi A., Ahmadi M.H., Qomi M.E., Kakoli E.: *MHD mixed convection and entropy generation in a 3-D microchannel using Al2O3–water nanofluid*. J. Taiwan Inst. Chem. Eng. **46**(2015), 30–42.

[14] Amirahmadi S., Rashidi S., Esfahani J.A.: *Minimization of exergy losses in a trapezoidal duct with turbulator, roughness and beveled corners*. Appl. Therm. Eng. **107**(2016), 533–543.

[15] Bianco V., Nardini S., Manca O.: *Enhancement of heat transfer and entropy generation analysis of nanofluids turbulent convection flow in square section tubes*. Nanoscale Res. Lett. **6**(2011), 1, 252.

[16] Behera T.R.: *Computational Study on Entropy Generation Minimization of Pipe Bending*. Phd thessis, National Institute of Technology Rourkela, Rourkela 2015.

[17] Shanbedi M., Zeinali H.S., Maskooki A., Eshghi H.: *Statistical analysis of laminar convective heat transfer of MWCNT-deionized water nanofluid using the response surface methodology*. Num. Heat Transfer A-Appl. **68**(2015), 4, 454–469.

[18] Shirvan K.M., Mamourian M., Mirzakhanlari S., Ellahi R.: *Two-phase simulation and sensitivity analysis of effective parameters on combined heat transfer and pressure drop in a solar heat exchanger filled with nanofluid by RSM*. J. Mol. Liq.**220** (2016), 888–901.

[19] Chan J.S., Ghadimi A., Simon H., Metselaar C., Lotfizadehdehkordi B.: *Optimization of temperature and velocity on heat transfer enhancement of non-aqueous alumina nanofluid*. J. Eng. Sci. Technology **10**(2015), 85–101.

[20] Darbari B., Rashidi S., Abolfazli Esfahani J.: *Sensitivity analysis of entropy generation in nanofluid flow inside a channel by response surface methodology*. Entropy **18**(2016), 2, 52.

[21] Esfandiary M., Habibzadeh A., Sayehvand H.: *Numerical study of single phase/two-phase models for nanofluid forced convection and pressure drop in a turbulence pipe flow*. Transp. Phenom. Nano Micro Scales **4**(2016), 1, 11–18.

[22] Launder B.E., Spalding D.B.: *The numerical computation of turbulent flows*. Comput. Meth. Appl. M. **3**(1974), 2, 269–289.

[23] Kays W.M., Crawford M., Weigang B.:*Convective Heat and Mass Transfer*. Tata McGraw-Hill Education, 2012

[24] Pak B.C., Cho Y.I.: *Hydrodynamic and heat transfer study of dispersed fluids with submicron metallic oxide particles*. Exp. Heat Transfer Int. J. **11**(1998)2, 151–170.

[25] Xuan Y., Roetzel W.: *Conceptions for heat transfer correlation of nanofluids*. Int. J. Heat Mass Trans.**43**(2000), 19, 3701–3707.

[26] Corcione M.: *Empirical correlating equations for predicting the effective thermal conductivity and dynamic viscosity of nanofluids*. Energ. Convers. Manage.**52**(2011), 1, 789–793.

[27] Saha G.: *Heat Transfer Performance Investigation of Nanofluids Flow in a Pipe*. Phd thesis, University of Glasgow, Glasgow 2016.

[28] Yunus A.C., Cimbala J.M.: *Fluid Mechanics: Fundamentals and Applications*. McGraw Hill Publ. 2006.

[29] Ratts E.B., Raut A.G.: *Entropy generation minimization of fully developed internal flow with constant heat flux*. J. Heat Transfer **126**(2004), 4, 656–659.

[30] Khuri A.I., Mukhopadhyay S.: *Response surface methodology*. WIREs Comp. Stat. **2**(2010), 2, 128–149.

[31] Bathe K.J.: *'ADINA theory and modeling guide.' Volume I: ADINA Solids and Structures*. ADINA R&D, Watertown, MA 2012.

[32] Fadodun O.G., Amosun A.A., Salau O.A., Ogundeji J.A., Olaloye D.O.: *Numerical investigation of thermal performance of single-walled carbon nanotube nanofluid under turbulent flow conditions*. Engineering Reports **1**(2019), 1, doi.org/10.1002/eng2.12024.

[33] Fadodun O.G., Amosun A.A., Okoli N.L., Olaloye D. O., Ogundeji J.A., Durodola S.S.: *Numerical investigation of entropy production in $SWCNT/H_2O$ nanofluid flowing through inwardly corrugated tube in turbulent flow regime*. J. Therm. Anal. Calorim. **4**(2020), 1–16.

[34] Fadodun O.G., Amosun A.A., Salau A.O., Olaloye D. O., Ogundeji J.A., Ibitoye F.I., Balogun F.A: *Numerical investigation and sensitivity analysis of turbulent heat transfer and pressure drop of Al_2O_3/H_2O nanofluid in straight pipe using response surface methodology*. Arch. Thermodyn. **41**(2020), 1, 3–30.

[35] Carley K.M., Kamneva N.Y., Reminga J.: *Response surface methodology*. CASOS Techn. Rep. CMU-ISRI-04-136. Carnegie Mellon Univ., Pittsburgh 2004.

[36] Fadodun O.G., Amosun A.A., Ogundeji J.A., Olaloye D.O.: *Numerical investigation of thermal efficiency and pumping power of Al_2O_3/H_2O nanofluid in pipe using response surface methodology*. J. Nanofluids **8**(2019), 7, 1566–1576.

[37] *Version 7.0.0. Stat-Ease*. Design Expert Inc., Minneapolis, 2005.

[38] Gnielinski V.: *New equations for heat and mass transfer in turbulent pipe and channel flow*. Int. Chem. Eng. **16**(1976), 1, 359–368.

[39] Blasius H.: *Das Aehnlichkeitsgesetz bei Reibungsvorgängen in Flüssigkeiten*. Mitteilungen über Forschungsarbeiten auf dem Gebiete des Ingenieurwesens **131**(1913), 3, 1-41 (in German).

[40] Shari K.: *How to get Started with Design Expert Software*. Stat-Ease Inc., 2013.

[41] Mark A., Pat W.: *Design of Experiment Simplified*. Productivity Inc., 2003.

[42] Richard B.: *Design Expert 7. Introduction*. Mathematics Learning Support Centre. 2007.

[43] Campolongo F., Braddock R.: *The use of graph theory in sensitivity analysis of model output: a second order screening method.* Reliab. Eng. Syst. Saf. **64**(1999), 1, 1–12.

[44] Yau C.: *R Tutorial with Bayesian statistics using Open-BUGS*. Amazon.com Services LLC, 2013.

[45] Griewank A., Walther A.: *Evaluating Derivatives: Principles and Techniques of Algorithmic Differentiation*. 2nd Edn. (Vol. 105). SIAM, Philadelphia 2008.

[46] Fadodun O.G., Salau A.O., Amosun A.A., Ibitoye F.I.: *Sensitivity analysis and evaluation of critical size of reactor using response surface methodology.* IJET **10**(2019), 4, 184–190.

[47] Fadodun O.G., Amosun A.A., Okoli N.L., Olaloye D. O., Durodola S.S., Ogundeji J.A.: *Sensitivity analysis of entropy production in Al_2O_3/H_2O nanofluid through converging pipe.* J. Therm. Anal. Calorim. **12**(2019), 1–14.